Graphene oxide produced from spent coffee grounds in electrospun cellulose acetate scaffolds for tissue engineering applications

Graphene oxide produced from spent coffee grounds in electrospun cellulose acetate scaffolds for tissue engineering applications

Adam Aberra Challa[a], Nabanita Saha[a,*], Piotr K. Szewczyk[b], Joanna E. Karbowniczek[b], Urszula Stachewicz[b], Fahanwi Asabuwa Ngwabebhoh[a], Petr Saha[a]

[a]*Centre of Polymer Systems, University Institute, Tomas Bata University in Zlin, Czech Republic*

[b]*Faculty of Metals Engineering and Industrial Computer Science, AGH University of Science and Technology, Krakow, Poland*

[*]*Corresponding author. E-mail address: nabanita@utb.cz (N. Saha).*

ABSTRACT

Biomaterials are widely used in the field of tissue engineering as coatings, scaffolds, or injectables. Since these materials need to be compatible with the biological conditions of the human body, improving the sources and methods of production for biomaterials call for continuous innovation. In this study, fibers were electrospun from cellulose acetate (CA) polymer solution using graphene oxide (GO) as a filler, for bone tissue engineering applications. The GO was synthesized from spent coffee grounds, a carbonaceous source that is discarded abundantly. A non-energy-intensive methodology was used for the production. CA with 5 wt% of GO nanoparticles was dissolved in a dimethylacetamide and acetone solvent mixture to produce the polymer solution. The nanofibrous scaffolds were tested for their morphological and mechanical properties as well as their biocompatibility. Scanning electron microscopy (SEM) results showed that electrospinning produced smooth nanofibers with very few beads. Fiber diameters decreased with the addition of GO nanoparticles. Mechanical testing showed that modified CA scaffolds exhibited an improved tensile strength of 115.75 kPa on average compared to the pristine ones. In addition, a cell culture study revealed that using graphene oxide as a modifier of the matrix is non-toxic and promoted cell growth. The oxygen-rich and hydrophilic nature of GO played a role in the biocompatibility of the produced fibers. In general, this study showed that agro-residual biomass can be used to produce and modify biomaterials. This aspect contributes to research on sustainable bio-composites and the effort in environmental conservation.

Keywords: Nanofibrous scaffolds, graphene oxide, biomass, electrospinning, tissue engineering

1. Introduction

Biomaterials that are utilized as basic materials for the construction of scaffolds play a significant role in bone tissue engineering. Scaffolds mimic the structure and function of the natural bone extracellular matrix that can provide a three-dimensional ($3D$) environment to stimulate the adhesion, proliferation, and differentiation of cells [**1-3**]. Moreover, a biomaterial, to be used in tissue engineering, is required to be biocompatible, mechanically durable, and biodegradable [**4**]. Hence, source polymers for such materials, need to possess such properties or should be able to be tunable

to those effects. One of these polymers is graphene oxide (GO). GO is one of the derivatives of graphene and is praised for its excellent properties such as electrical conductivity, mechanical strength, and optical properties. It also proves to be effective in osteogenesis and promotes cell differentiation and adhesion, hence has good biocompatibility features [**5**]. GO is also a remarkable material to enhance the properties of other biopolymers by forming bio-composite scaffolds [**6**].

The two widely used methods to synthesize GO are the bottom-up and the top-down approaches [**7**]. The bottom-up approach involves chemical vapor deposition and epitaxial growth of graphene, whereas the top-down approach includes methods such as liquid-phase exfoliation and micromechanical cleavage [**8**]. The main source of GO, used in the second approach, is graphite. Nowadays, due to the increasing need for GO in the research and industry sector, the production and the amount of graphite needed is highly growing. However, both natural and synthetic sources of graphite pose challenges. Technical and economic hindrances, especially for large-scale applications are very significant [**9**]. Effects on the environment during sourcing and production are also a current concern [**10**].

Thus, research is being done to synthesize GO from natural sources. For example, agricultural or forest biomass that contains cellulose, hemicellulose, and lignin are known to be carbonaceous and hence are now being used to synthesize GO [**11**]. One of these is ground coffee waste.

Coffee is one of the most widely consumed beverages in the world next to water. In the year 2020/2021 alone, around 11 million tons of coffee were consumed worldwide [**12**]. This makes it a product that attracts diversified attention worldwide. Producers earn fortunes, consumers take caffeine whereas researchers study it further. However, after brewed coffee is used, what remains is wet spent coffee grounds twice the weight of the powder used [**13**]. This waste is largely discarded into landfills or water bodies. Due to the acidic nature of ground coffee, especially that of the most used arabica coffee, this unmanaged leftover would induce acidity in the soil and endanger aquatic nature. It also releases methane into the environment [**14**]. For several years, the portion of the ground coffee waste that remained from being thrown has been used to produce biofuel, fertilizers, and recycled utensils [**15,16**]. This phenomenon inhibited the great potential of a product this big.

Spent coffee grounds are mainly composed of 12.4% cellulose, 39.1% hemicellulose (3.6% arabinose, 19.07% mannose, 16.43% galactose), and 23.9% lignin [**17**]. This composition makes coffee grounds rich in carbon, an element that can be extracted through physical and chemical processes, and hence potential sources of biomaterials or biopolymers due to the advantage of biodegradability [**18,19**]. Thus, utilizing these sources for GO production is viable in this regard.

Another biomaterial currently being used in tissue engineering is cellulose acetate (CA). CA is a bio-polymer that has been used extensively for its excellent biocompatible properties. It shows a promising role in tissue engineering, because of its ability to promote osteoblast proliferation and osteogenic cell differentiation [**20**].

Unfortunately, even though CA is easy to produce, can be renewable, and has proven to be non-toxic, it cannot be used for tissue engineering in its pristine form. This is because it possesses low mechanical strength [**21**]. Fibers, films, porous bulks, and asymmetric membranes produced from CA exhibit poor structural stability [**5**]. This phenomenon makes it unable to mimic the in-vivo conditions required for a bone graft in bone tissue engineering.

To utilize the best properties of CA as a biopolymer in tissue engineering, producing bio-composite materials has proved to be a good technique. By combining CA with synthetic polymers such as polyvinyl pyrrolidone, and polylactic acid, or natural polymers such as collagen and pullulan, for their better mechanical properties and adjustable biocompatibilities, studies show that improved $3D$ scaffolds were produced [**22**]. However, innovations for easy-produced and sustainable modifiers remain challenging. To address this issue, studies are being made by incorporating GO into a CA polymer mixture to produce scaffolds to mimic bone grafts using the electrospinning technique.

Electrospinning is a technique that is widely used to produce fiber matrices and scaffolds [**23**]. It gives an alternative approach to producing micro- and nanofibers. By adjusting the required parameters, fabricating aligned or non-aligned fiber matrices is also possible. These fiber matrices have several applications including membrane processing, bio-medical applications, sensors, and electrical system [**24**]. They can also be ingeniously used for water filtration [**25**], water [**26**], and energy harvesting [**27,28**]. The use of electrospinning in producing materials for biomedical applications [**29**], tissue engineering [**30,31**] in specific, is now a widely shared interest.

Electrospinning CA/GO solution not only produced beads-free but also resulted in an impressive boost in tensile strength compared to pristine CA fibers [**32**]. A study on cancer cells seeded onto GO/CA scaffolds resulted in higher viability and better cell adhesion than when CA was used alone [**33**].

This study focused on the production of electrospun nanofiber scaffolds from CA/GO polymer bio-composite. The CA was dissolved in a dimethylacetamide/acetone mixture. The GO added to the polymer solution was produced from spent coffee grounds instead of its conventional source (graphite), which is the novelty of this research. Using such an alternative means cuts down the environmental risk contribution of using graphite as a source, utilizing the potential of the abundant waste at the same time. The GO particles were used as modifiers for the improvement of the properties of the CA nanofibers. After the production of CA/GO scaffolds, the characterization of the said biomaterial and cell studies was checked for potential applications in tissue engineering.

2. Materials and methods

2.1. Materials for scaffold preparation

For producing graphene oxide (GO), coffee waste was collected from used Arabica ground coffee; 98% pure sulfuric acid (H_2SO_4), sodium nitrate ($NaNO_3$), potassium permanganate ($KMnO_4$), sodium hydroxide (NaOH), and 30% pure hydrogen peroxide (H_2O_2), were purchased from Sigma-Aldrich, Czech Republic. To produce the scaffold fibers, cellulose acetate (CA, average $Mn \approx$ 50,000 by GPC, Sigma Aldrich, USA) was used, as a supporting polymer matrix. To dissolve the polymer, a mixture of dimethylacetamide (DMAc) and acetone was used (purchased from Sigma Aldrich, USA).

2.2. Synthesis of graphene oxide (GO)

The ground coffee waste was put in an oven at 50 °C for 24 h. For carbonization, 5 g of the sample was heat-treated in a tube furnace at 700 °C for 4 h under argon gas flow. The resulting black char was used as a precursor to synthesize GO using the Modified Hummer's method [**34**]. To conduct the Hummer's method, 2 g of the carbonized biochar was mixed with 50 ml of H_2SO_4 in an ice bath. One gram of $NaNO_3$ was slowly added and the mixture is constantly stirred for 4 h. Then, 6 g of $KMnO_4$ was added to the solution as an oxidizing agent, keeping the temperature below 20 °C. After 1 h of stirring, the

ice bath was removed, and the stirring continued for another hour at 35 °C. Then, 100 ml of deionized water was added carefully, and the mixture is stirred at 90 °C for an hour. Afterward, 200 ml of deionized water was added followed by 10 ml of 30% H_2O_2 to stop the reaction. Then the solution was centrifuged at 8000 rpm to remove impurities. This was decanted and the remaining sample was washed with deionized water. Finally, the sample was ultrasonicated for 1 h.

2.3. Characterization of GO

A Scanning electron microscope (SEM, Merlin Gemini II, Zeiss, Germany) was used to check the morphological structure of the GO particles after the sample was coated with an 8 nm gold layer using rotary pump sputter coater (Q150RS, Quorum Technologies, United Kingdom). Raman (Thermo Scientific, Nicolet DXR, Czech Republic) spectroscopy was used to investigate the chemical structure of the molecules. Fourier Transform Infrared (FTIR) spectroscopy in an Attenuated Total Reflectance (ATR) mode (Thermo Scientific, Nicolet iS5, Czech Republic) was utilized to study different functional groups in the samples. The spectra were measured in wavelengths of 4000-400 cm^{-1}.

2.4. Preparation of electrospun (CA/GO) scaffold

Pristine CA polymer solution was prepared by using a 1:1 vol ratio of DMAc: Acetone solvent mixture. CA powder was dried overnight at 50 °C and added at a concentration of 19 wt% of the solution. This was homogenized in an ultrasonic bath (Sonorex Bandelin, Germany) for 30 min and followed by an overnight stirring in a magnetic steerer ($IKA\ RCT$ basic, Staufen, Germany) at a speed of 150 rpm. The solution was ultrasonicated again for 2 h, before electrospinning.

CA/GO polymer solution was prepared using the same solvent mixture. GO was added to the solvent at a concentration of 5 wt% of the polymer (CA). This was ultrasonicated for 1 h. Afterward, CA was added at 15 wt% concentration of the total solution. A 30 min ultrasonication followed to better disperse the particles. Then a similar procedure was used before electrospinning.

Electrospinning was performed in an $EC-DIG$ (IME Technologies, Waalre, The Netherlands) apparatus. The electrospinning parameters were set for optimal cellulose acetate fibers. The environmental conditions for electrospinning were set at 25 °C and 65-70% humidity. Flowrate was maintained at 0.1 mlh^{-1}. A 13 kV high voltage was applied to the nozzle kept 20 cm away from the collecting drum. The electrospun fibers were collected on Al foil for SEM images, paper frames for mechanical testing, and glass slides for cell culture studies.

2.5. Characterization of scaffolds

The morphology of the scaffolds was studied using scanning electron microscopy (SEM, Merlin Gemini II, Zeiss, Germany). All samples were coated with an 8 nm gold layer using a rotary pump sputter coater (Q150RS, Quorum Technologies, United Kingdom). Fibers' diameters were measured from SEM micrographs by ImageJ software (ver. 1.53c, USA) by taking 100 measurements for each sample. To investigate the presence of GO particles in the CA nanofibers, Raman spectroscopy (Thermo Scientific, Nicolet DXR, Czech Republic) was employed. A wettability test was conducted by placing 3 μl deionized (DI) water (distilled using Spring 5 UV purification system—Hydrolab, Straszyn, Poland) droplets on the fiber surfaces. The images were taken by a Canon EOS 700D camera with EF-S 60 mm f/2.8 Macro USM zoom lens. Water contact angle of droplets was measured using ImageJ software

[**35**]. Tensile strength measurements took place using a tensile module equipped with a 1 N (load resolution 1 x 10^{-5} N) load cell (B.1708. A, Kammrath & Weiss, Dortmund, Germany). Strips of fibers (20 x10 mm) were laser-cut from the fibers collected on paper and carefully placed on clamps of the module. The strain rate on the module was set at 25 |rm/min. This load-elongation data was analyzed using the results of five measurements for both test samples. The stress-strain graphs were then drawn using Origin software (ver. 2021, USA). Cross-sections of fibers deposited on paper frames were imaged by SEM. The average thickness was taken based on 5 measurements of the SEM images [**36**].

2.6. Biocompatibůity study

Human osteoblast-like cell line MG-63 (Sigma-Aldrich, United Kingdom) was used for cell proliferation studies. For cell detaching, Trypsin $EDTA$ solution and for preparation of cell culture medium, Fetal Bovine Serum (FBS), Dulbecco's Modified Eagle Medium ($DMEM$), MEM-Eagle solution, a mixture of Penicillin and Streptomycin and L-Glutamine solution were purchased from Biological Industries, Israel. Cell viability test was done using Cell Titer-Blue® Assay (Promega, United States). For SEM imaging, glutaraldehyde (Sigma Aldrich, United Kingdom) was used.

2.7. Cell culture studies

The scaffolds from electrospun fibers were collected on circular glass slides and were first sterilized under UV light for 30 min. The MG-63 cells were washed with PBS. Trypsin was used to detach the cells from their plate. Fresh cell culture media was then prepared containing 86% $DMEM$, 1% MEM-Eagle (as an amino acid), 10% FBS, 2% mixture of Penicillin & Streptomycin (as an antibiotic), and 1% L-Glutamine solution. The cells were seeded in this media at a concentration of 2 x 104 cells per 1 ml of media and placed on the scaffolds. These samples were then incubated under 37 °C, and 90% humidity in CO_2 incubator (Memmert, Germany) [**31**].

Cell viability tests were undertaken after 1, 3, and 7 days using the Cell Titer-Blue® Assay. Glass slides were used as control. On those days, the samples were carefully transferred to new plates and the media was replaced with 480 il of fresh media containing 80 il of Cell Titer-Blue® reagent, followed by incubation for 4 h at 37 °C. The proliferation was checked by fluorescence reading at 520 nm using the microplate reader GloMax® Discover System (Promega, United States).

For SEM Imaging, cells on the scaffolds were transferred to new plates and washed with PBS after 3, and 7 days of growth. They were then fixed with 2.5% glutaraldehyde for 1 h at 23 °C. After removing the glutaraldehyde, they were washed three times with PBS and dehydrated in a series of ethanol solutions. The samples were attached on Al holders by carbon tape and gold-sputtered with an 8 nm layer using a rotary pump sputter coater (Q150RS, Quorum Technologies, United Kingdom). Finally, the samples were analyzed using SEM [**37**].

Statistical analysis of cell proliferation results was done using oneway analysis of variance ($ANOVA$) followed by Tukey' s post hoc test in Origin Pro (ver. 2021, USA) where the statistical significance was evaluated at $p < 0.01$.

3. Results and discussion

3.1. Synthesis of GO

GO particles were successfully synthesized from ground coffee waste using the modified Hummer's method [**34**]. The $KMnO_4$ played a role as the oxidizing agent for the carbonized precursor. The morphology of the particles was checked using SEM images (given in **Fig. S1**). It was observed that the particle sizes were lowered to the nanoscale with increased ultrasonication. This can be greatly attributed to the alteration in the number of GO sheet layers through ultrasonication treatment [**38**].

Fig. 1a gives the Raman spectra for the GO particles. The D and G bands on the spectra appear at 1339 cm^{-1} and 1598 cm^{-1} respectively. These are typical for GO where the D band indicates the breathing mode of aromatic rings whereas the G band corresponds to $C—C$ stretching [**39,40**]. Another peak appeared at 2770 cm^{-1}, indicating a 2D band which verifies that there is a multiple-layer stacking of graphene sheets [**41**]. The ultrasonication step utilized in Hummer's method was crucial to obtain the exfoliated GO sheets.

$FTIR$ spectroscopy of the particles also confirms the formation of GO. As can be seen in **Fig. 1**b, oxygen-containing groups such as hydroxyl groups (-OH stretching vibration) at 3400 cm^{-1}, carbonyl groups ($C=O$ stretching vibration) at 1715 cm^{-1}, and epoxy groups ($C-O-C$) at 1065 cm^{-1} were formed. The peak seen at 1600 cm^{-1} can be assigned to $C-C$ stretching and absorbed hydroxyl groups, whereas the peak at 1235 cm^{-1} shows the $C-O$ bond. An aliphatic bond ($C-H$) was formed at 2900 cm^{-1}. These peaks match with characterizations done by previous studies which synthesized GO using the modified Hummer' s method [**42-44**]. However, variations in the exact wavenumber exist since our GO is produced from a different precursor and not graphite. The synthesized GO was then used to modify the CA solution prepared for electrospinning.

The possibility of producing GO from a sustainable source such as coffee grounds is a promising aspect. The conventional source, graphite, mostly requires mining which exploits the natural environment. In addition, given that its production involves heavy machinery for mining, milling and graphitization processes, it proves to be a highly industrialized chain [**45**]. Compared to this, utilizing the easy-to-use agro-waste instead, in a manner shown above, eliminates the use of many of the machineries, energy and additional compounds needed in the former.

The synthesized GO was then used to modify the CA solution prepared for electrospinning.

3.2. Electrospun CA scaffolds with GO

The result of 2 h of electrospinning is shown as a fibers' mesh in **Fig. S2** in the supporting information. SEM studies revealed the morphology, indicating very minimal beads on nanofibers, see **Fig. 2**. Other than the effect of the set environmental parameters in the electrospinning chamber [**46**], the addition of GO particles also helped in minimizing the formation of beads. This is mainly due to the higher viscosity and conductivity induced by the particles [**47,48**]. The fibers have nearly similar diameters with a slightly decreasing size with the addition of GO. The average diameter of the pristine CA fibers as shown in **Fig. 2**a was measured to be 458 ± 158 nm. The decrease in fiber diameter to 329 ± 137 nm in **Fig. 2**b is related to the decomposition of amorphous carbon in the carbonization stage of synthesizing the GO [**49**]. The histograms shown in **Fig. 2**c show the distribution of diameters of the nanofibers. Additionally, the images reveal that the morphology of the fibers' surface is smooth with very minimal defects. Fibers run breakage-free along their lengths. This is also true for the fibers containing the GO particles. These findings match those reported in other studies as well [**50,51**].

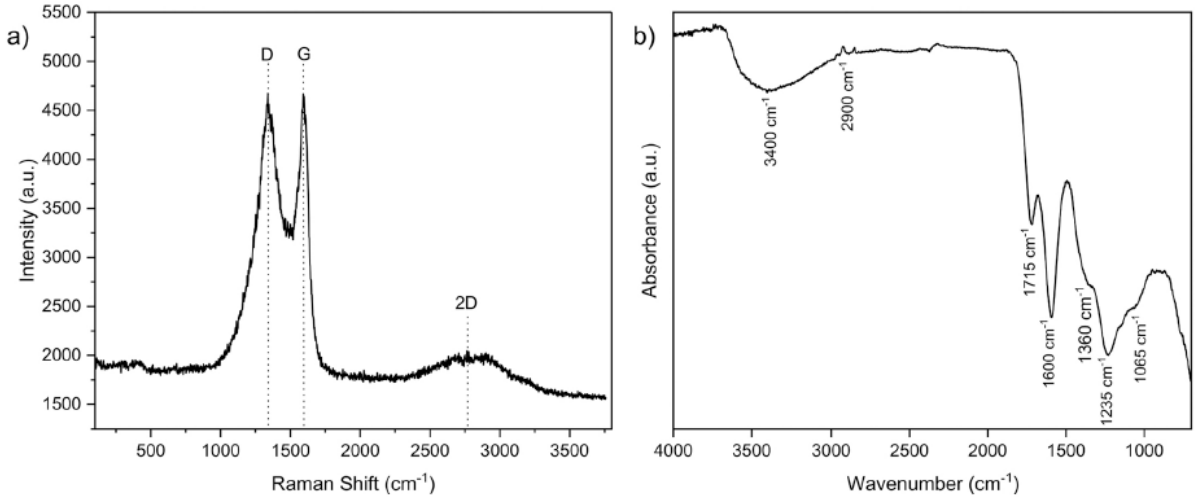

Fig. 1. Characterization of the synthesized GO a) Raman spectra and b) $FTIR$ spectra.

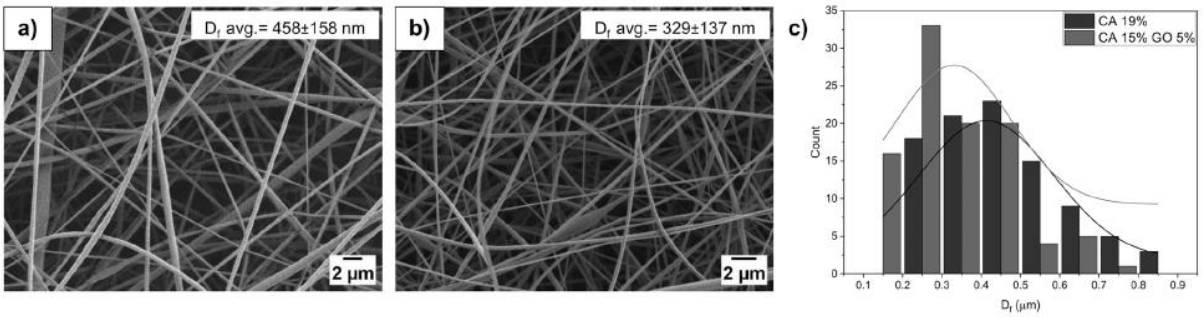

Fig. 2. SEM images of nanofibrous scaffolds produced from (a) pristine CA and (b) CA/GO mixture (c) with their respective diameter histograms.

SEM images confirmed that GO particles are incorporated in the CA fibers, as indicated in **Fig. 3**.

In further analysis of the CA/GO interactions using Raman spectroscopy, as seen in **Fig. 4**, we were able to depict a peak (G band) in the CA/GO graph, at a wavelength that is a signature for that of GO. The peak does not appear on the pristine CA graph. This clarifies the GO's presence in the nanofibers produced.

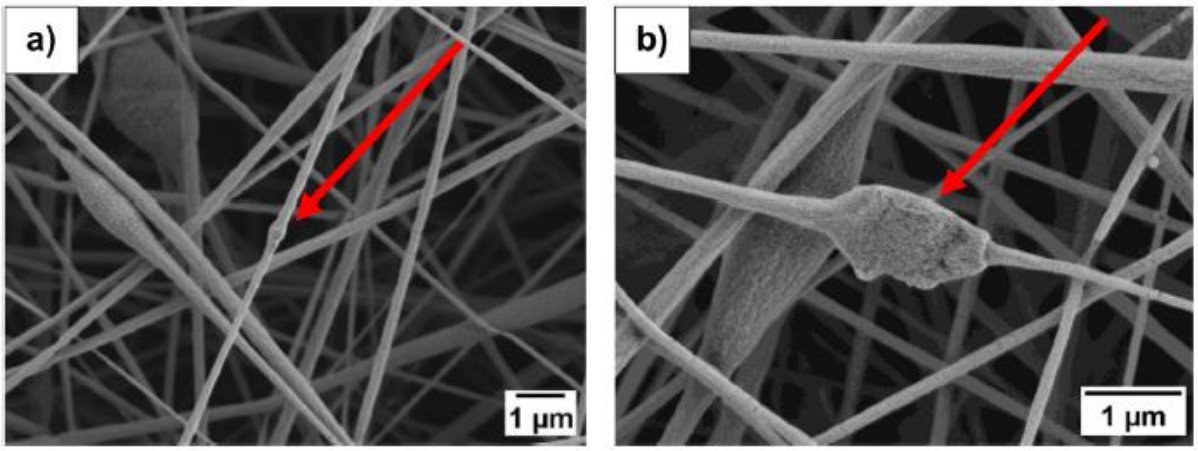

Fig. 3. a-b. SEM micrographs of CA nanofibers with embedded GO nanoparticles indicated with the red arrows, where a) and b) are taken at different locations.

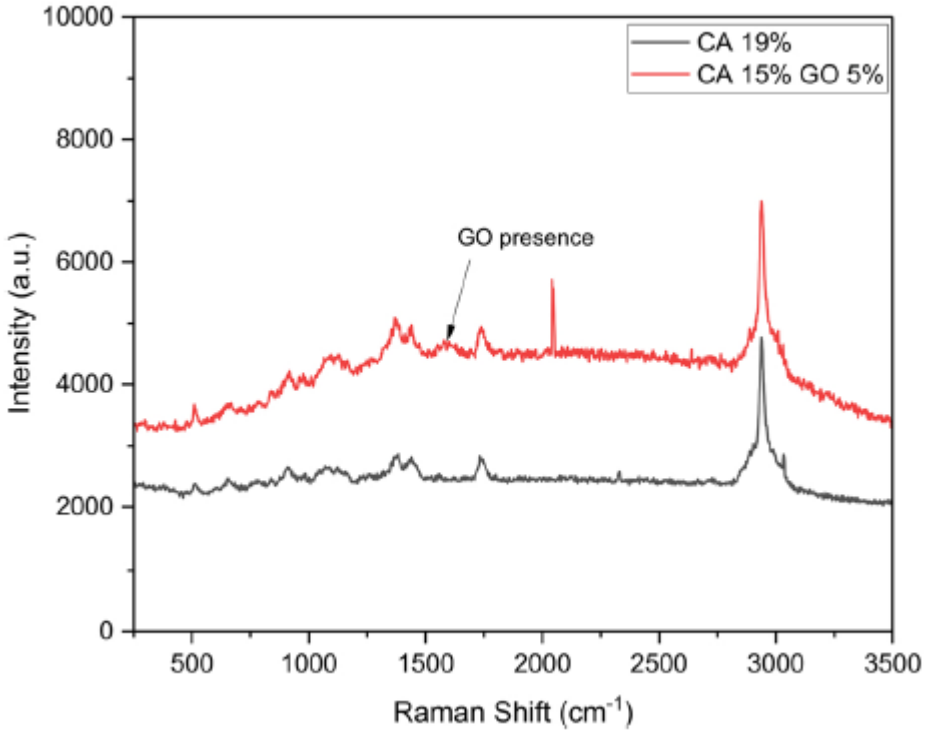

Fig. 4. Raman spectra of nanofibrous scaffolds with and without GO particles indicated by the Raman shift at 1592 cm^{-1} for GO presence.

3.3. Water contact angle

A wettability test was carried out and indicated a decrease in hy-drophobicity of the fibers through the addition of GO. It was observed that the contact angle decreased from 139.18 $\pm$ 3.59° to 125.48 $\pm$ 9.69°. GO is known to be a hydrophilic compound due to its -OH functional groups [**52**]. This has proven to be the case in our study (see **Fig. S3**). Studies show that the wettability behavior of electrospun fibers improves cell attachment and subsequent cell spreading when used in skin treatment or tissue engineering purposes [**53**]. Thus, it can be seen that the GO particles' effect on reducing the hydrophobicity of the CA scaffolds could help in the cell proliferation stages.

3.4. Mechanical strength

Prior to the calculation of the tensile strength of the fibers, the thicknesses of the scaffolds were measured using SEM and the measurements were 19.42 pm for the pristine CA scaffold and 17.04 μm for CA scaffold with 5 wt% GO. The thicknesses of the samples were controlled via electrospinning time in both cases. In **Fig. S4**, the samples attached to the tensile module clamps are presented.

The tensile stress-strain curve for the scaffolds with and without GO is given in **Fig. 5**. As can be seen, the average tensile strength increased from 101.3 kPa to 115.75 kPa through the addition of GO, at a concentration of 5 wt% of CA. All the individual stress-strain curves are given in **Fig. S5** in the supporting information. With the increasing application of the load, the fibers gradually aligned themselves in a regular order. The 14.2% rise in the tensile strength of the nanofibers is largely due to intermolecular hydrogen bonding formed through hydrogen-containing functional groups (-$COOH$, -

OH) which the GO particles possess [**54,55**]. The presence of these functional groups in the GO particles has been indicated in the $FTIR$ spectra in **Fig. 1**b of this study.

Through this process, it was observed that there was a sudden loss in strength of the fibers shown by the vertical drop on the stress curve. This happened at around 25% strain of most of the fibers. This was probably due to the deformational characteristics of the breaking fibers, as indicated in previous studies [**56**] [**57**]. Upon loading, fibers aligned in the longitudinal axes of the sample contribute the highest to the strength of the scaffolds. The other fibers that are not in such alignment tend to slip from their axis as elongation increases. Thus, they would break at a load less than the ultimate tensile load for the sample [**58**].

On the other hand, the mechanical measurement revealed that the strain at the break of the CA/GO fibers is less than that of the pristine CA. This is attributed to the low fracture strength that GO possesses. The same interactions among functionalized carbon atoms result in crack inhibition [**59**].

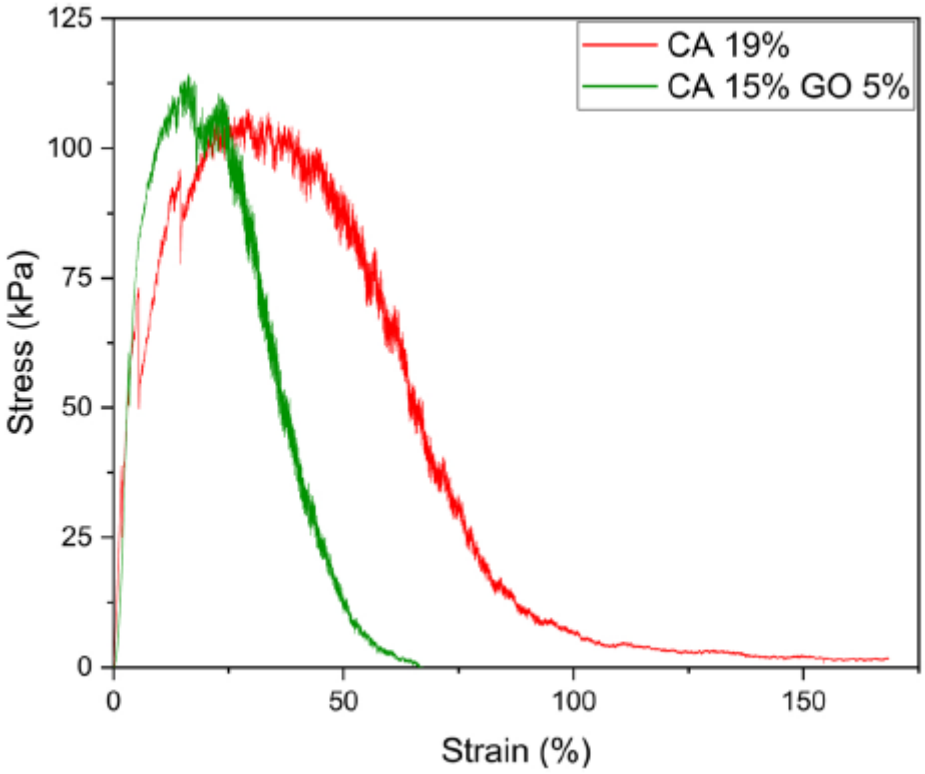

Fig. 5. The representative stress-strain curve for the tensile tested electrospun random fibers' mesh with pristine CA and CA/GO mixture.

3.5. Cell culture studies

The main aspect of electrospinning in tissue engineering is to mimic the extracellular matrix in living tissues by producing fibrous structures. These structures or scaffolds become complex when they are made from bio-composites like the subject of this study. Hence the need for cell culture study is imperative. The biocompatibility test for our study was done after 1, 3, and 7 days. Enough fresh media for the cells was ensured by replacing the media after every 2 days. The cell proliferation was checked on the indicated days using the microplate reader. From the cell proliferation result depicted in **Fig. 6**a, cellulose acetate is found to be conducive to the growth of osteoblast cells. This result matches

previous findings [**60**]. The main aspect of this biocompatibility test was to check the cytotoxicity of the fibers modified with GO. The fibers with GO proved to be non-toxic to the MG 63 cells, as the cell viability is more than 70% compared to the control (glass specimen). This is consistent with previous studies that show cell viability of GO modified polymers [**61,62**].

A biomaterial for tissue engineering not only needs to be mechanically strong and non-toxic but also conducive to cell proliferation. On the cell proliferation assay, it is clear that a significant amount of cell growth was registered on the 3rd and 7th days of incubation. To further investigate this, SEM imaging was used to identify the growth of cells on the nanofibrous scaffolds. **Fig. 6**b-e show the attachment of cells. As can be seen, the pristine CA scaffolds in **Fig. 6**b and c experienced a wider spreading of the cells. CA/GO nanofiber scaffolds also promoted the attachment and spreading of the MG-63 cells as shown in **Fig. 6**d and e. The oxygen-rich nature, hydrophilicity, and flexibility of GO promote cell growth and expansion when used in tissue regeneration [**63**]. Moreover, GO particles have an advantage in bone tissue engineering applications since they increase the stem cells located in the bone which play an important role in bone repair and growth [**64**]. Thus, it is a vital approach to use GO as a modifier for the CA fibers. Although, it is important to note that using a higher concentration of GO might lead to a negative effect on biocompatibility, as has been indicated in a previous study [**65**].

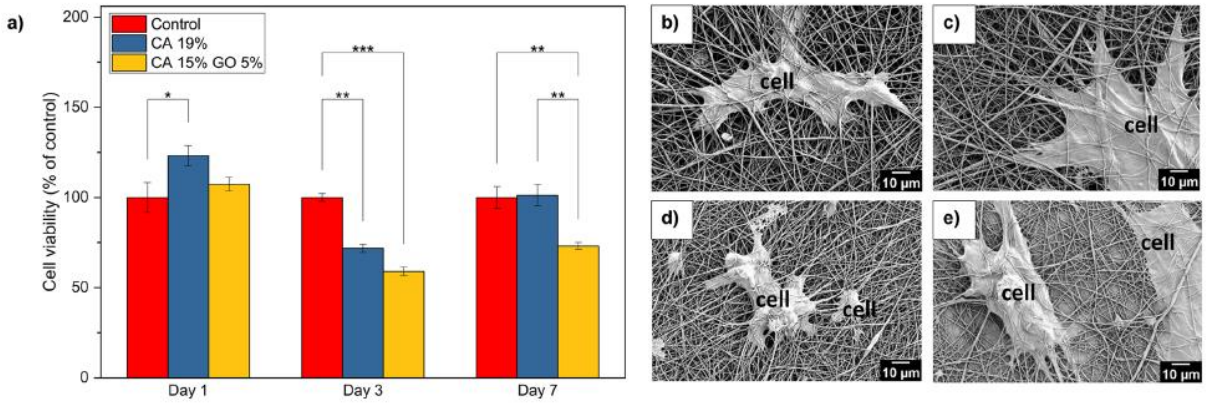

Fig. 6. Cell proliferation result from Cell Titer-Blue® assay (statistical significance calculated with $ANOVA$ followed by Tukey's post hock tests; $^{*}p <=0.05$, $^{**}p <=0.01$, $^{***}p <=0.001$) (a); SEM micrographs of cell spreading on pristine CA scaffolds on day 3 (b) & day 7 (c) and on CA/GO scaffolds on day 3 (d) & day 7 (e).

4. Conclusions

Graphene oxide nanoparticles were produced from agro-residual biomass, i.e., ground coffee waste. This was achieved through sustainable, non-energy-intensive means, proving that abundant day-to-day waste can be used to produce biomaterials needed for complex applications. This achievement provides a means of reducing/eliminating the environmental impact that producing its conventional source, graphite, has. The synthesized GO particles were dissolved in a CA polymer solution to produce nanofibrous scaffolds for its use in tissue engineering. Analysis of the electrospun fibers showed that GO particles were embedded in the CA fibers and helped reduced the fiber diameters by 28%. The mechanical properties of the scaffolds were improved through the addition of the GO particles, measuring a 14.2% increase in average tensile strength. This alleviated the strength shortcomings of the widely used biopolymer, CA. Moreover, the introduction of GO nanoparticles to the CA fiber matrix proved to be non-cytotoxic and instead promoted the adhesion and proliferation of cells.

This study contributes to the knowledge of modifying biopolymers for tissue engineering purposes by using modifiers from sustainable sources. The spent coffee grounds used here underline the prospect of maintaining ecological balance through waste management. On top of that, the synthesized GO particles and the subsequent fibers performed as expected. Thus, we believe this study creates a valuable link between the conservation of the environment and the effective production of biomaterials. We further hope that it opens more ideas for researchers in the quest of improving the use of biomaterials in the healthcare sector.

References

[1] S. Bhushan, et al., Scaffold fabrication techniques of biomaterials for bone tissue engineering: a critical review, Bioengineering 9 (2022), **https://doi.org/10.3390/ bioengineering9120728**.

[2] M. Filippi, et al., Natural polymeric scaffolds in bone regeneration, Front. Bioeng. Biotechnol. 8 (2020).

[3] H. Qu, et al., Biomaterials for bone tissue engineering scaffolds: a review, RSC Adv. 9 (45) (2019) 26252-26262.

[4] L. Daneshmandi, et al., Graphene-based biomaterials for bone regenerative engineering: a comprehensive review of the field and considerations regarding biocompatibility and biodegradation, Adv. Healthc. Mater. 10 (1) (2021) 2001414.

[5] S.-R. Ignat, et al., Versatile biomaterial platform enriched with graphene oxide and carbon nanotubes for multiple tissue engineering applications, Int. J. Mol. Sci. (2019) **20**, **https://doi.org/10.3390/ijms20163868**.

[6] P.R. Sivashankari, et al., Graphene oxide-reinforced pectin/chitosan polyelectrolyte complex scaffolds, J. Biomater. Sci. Polym. Ed. 32 (17) (2021) 2246-2266.

[7] M. CORO, et al., A brief overview on synthesis and applications of graphene and graphene-based nanomaterials, Front. Mater. Sci. 13 (1) (2019) 23-32.

[8] Z. Ismail, Green reduction of graphene oxide by plant extracts: a short review, Ceram. Int. 45 (18, Part A) (2019) 23857-23868.

[9] S. Lowe, Y.L. Zhong, Challenges of Industrial-Scale Graphene Oxide Production: Fundamentals and Applications, 2016, pp. 410-431.

[10] R.B. Capaz, Grand challenges in graphene and graphite research, Front. Carbon 1 (2022).

[11] E. Thompson, et al., Iron-catalyzed graphitization of biomass, Green Chem. 17 (1) (2015) 551-556.

[12] ICO, Coffee Consumption Worldwide from 2012/13 to 2020/21 (in Million 60kg Bags) 2021 January 31, 2021]; Available from: (**https://www.statista.com/statisti cs/292595/global-coffee-consumption/**).

[13] A. Colantoni, et al., Spent coffee ground characterization, pelletization test and emissions assessment in the combustion process, Sci. Rep. 11 (1) (2021) 5119.

[14] A. Mukherjee, et al., Carbon dioxide capture from flue gas in biochar produced from spent coffee grounds: effect of surface chemistry and porous structure, J. Environ. Chem. Eng. 9 (5) (2021), 106049.

[15] N. Kondamudi, S.K. Mohapatra, M. Misra, Spent coffee grounds as a versatile source of green energy, J. Agric. Food Chem. 56 (24) (2008) 11757-11760.

[16] J. McNutt, Q. He, Spent coffee grounds: a review on current utilization, J. Ind. Eng. Chem. 71 (2019) 78-88.

[17] L.F. Ballesteros, J.A. Teixeira, S.I. Mussatto, Chemical, functional, and structural properties of spent coffee grounds and coffee silverskin, Food Bioprocess Technol. 7 (12) (2014) 3493-3503.

[18] L. Jenícek, et al., Use of spent coffee ground as an alternative fuel and possible soil amendment, Materials (2022) 15, **https://doi.org/10.3390/ma15196722**.

[19] K.Y. Sen, S. Baidurah, Renewable biomass feedstocks for production of sustainable biodegradable polymer, Curr. Opin. Green Sustain. Chem. 27 (2021), 100412.

[20] N.Z. Shaban, et al., Cellulose acetate nanofibers: incorporating hydroxyapatite (HA), HA/berberine or HA/moghat composites, as scaffolds to enhance in vitro osteoporotic bone regeneration, Polymers (2021) 13, **https://doi.org/10.3390/ polym13234140**.

[21] H. Kamal, F.M. Abd-Elrahim, S. Lotfy, Characterization and some properties of cellulose acetate-co-polyethylene oxide blends prepared by the use of gamma irradiation, J. Radiat. Res. Appl. Sci. 7 (2) (2014) 146-153.

[22] M. Janmohammadi, et al., Cellulose-based composite scaffolds for bone tissue engineering and localized drug delivery, Bioact. Mater. 20 (2023) 137-163.

[23] B.A. Chinnappan, et al., Electrospinning of biomedical nanofibers/ nanomembranes: effects of process parameters, Polymers (2022) 14, **https://doi. org/10.3390/polym14183719**.

[24] R. Beigmoradi, A. Samimi, D. Mohebbi-Kalhori, Fabrication of polymeric nanofibrous mats with controllable structure and enhanced wetting behavior using one-step electrospinning, Polymer 143 (2018) 271-280.

[25] I. Tlili, T.A. Alkanhal, Nanotechnology for water purification: electrospun nanofibrous membrane in water and wastewater treatment, J. Water Reuse Desalin. 9 (3) (2019) 232-248.

[26] J. Knapczyk-Korczak, U. Stachewicz, Biomimicking spider webs for effective fog water harvesting with electrospun polymer fibers, Nanoscale 13 (38) (2021) 16034-16051.

[27] P.K. Szewczyk, et al., Enhanced piezoelectricity of electrospun polyvinylidene fluoride fibers for energy harvesting, ACS Appl. Mater. Interfaces 12 (11) (2020) 13575-13583.

[28] T. Busolo, et al., Triboelectric yarns with electrospun functional polymer coatings for highly durable and washable smart textile applications, ACS Appl. Mater. Interfaces 13 (14) (2021) 16876-16886.

[29] Z.J. Krysiak, et al., Stretchable skin hydrating PVB patches with controlled pores' size and shape for deliberate evening primrose oil spreading, transport and release, Biomater. Adv. 136 (2022), 212786.

[30] U. Stachewicz, et al., 3D imaging of cell interactions with electrospun PLGA nanofiber membranes for bone regeneration, Acta Biomater. 27 (2015) 88-100.

[31] J.E. Karbowniczek, et al., Enhanced cells anchoring to electrospun hybrid scaffolds with PHBV and HA particles for bone tissue regeneration, Front. Bioeng. Biotechnol. (2021) 9.

[32] X. Liu, et al., Accelerated biomineralization of graphene oxide - incorporated cellulose acetate nanofibrous scaffolds for mesenchymal stem cell osteogenesis, Colloids Surf. B Biointerfaces 159 (2017) 251-258.

[33] Y. Wan, et al., Effect of graphene oxide incorporation into electrospun cellulose acetate scaffolds on breast cancer cell culture, Fibers Polym. 20 (8) (2019) 1577-1585.

[34] N.I. Zaaba, et al., Synthesis of graphene oxide using modified hummers method: solvent influence, Procedia Eng. 184 (2017) 469-477.

[35] P.K. Szewczyk, et al., Roughness and fiber fraction dominated wetting of electrospun fiber-based porous meshes, Polymers 11 (2019), **https://doi.org/ 10.3390/polym11010034**.

[36] J.E. Karbowniczek, D.P. Ura, U. Stachewicz, Nanoparticles distribution and agglomeration analysis in electrospun fiber based composites for desired mechanical performance of poly(3-hydroxybuty-rate-co-3-hydroxyvalerate (PHBV) scaffolds with hydroxyapatite (HA) and titanium dioxide (TiO2) towards medical applications, Compos. Part B Eng. 241 (2022), 110011.

[37] D.P. Ura, et al., Cell integration with electrospun PMMA nanofibers, microfibers, ribbons, and films: a microscopy study, Bioengineering 6 (2) (2019).

[38] G.T.T. Le, et al., Insight into the ultrasonication of graphene oxide with strong changes in its properties and performance for adsorption applications, Chem. Eng. J. 373 (2019) 1212-1222.

[39] F.T. Johra, J.-W. Lee, W.-G. Jung, Facile and safe graphene preparation on solution based platform, J. Ind. Eng. Chem. 20 (5) (2014) 2883-2887.

[40] V. Scardaci, G. Compagnini, Raman spectroscopy investigation of graphene oxide reduction by laser scribing, C 7 (2021), **https://doi.org/10.3390/c7020048**.

[41] N.H. Md Said, et al., Comparison on graphite, graphene oxide and reduced graphene oxide: synthesis and characterization, AIP Conf. Proc. 1892 (2017), 150002.

[42] E. Aliyev, et al., Structural characterization of graphene oxide: surface functional groups and fractionated oxidative debris, Nanomaterials 9 (2019), **https://doi.org/ 10.3390/nano9081180**.

[43] K. Krishnamoorthy, et al., The chemical and structural analysis of graphene oxide with different degrees of oxidation, Carbon 53 (2013) 38-49.

[44] D. Prodan, et al., Synthesis and characterization of some graphene oxide powders used as additives in hydraulic mortars, Appl. Sci. 11 (2021), **https://doi.org/ 10.3390/app112311330**.

[45] D. Surovtseva, et al., Toward a life cycle inventory for graphite production, J. Ind. Ecol. 26 (3) (2022) 964-979.

[46] P.K. Szewczyk, U. Stachewicz, The impact of relative humidity on electrospun polymer fibers: from structural changes to fiber morphology, Adv. Colloid Interface Sci. 286 (2020), 102315.

[47] C. Huang, et al., Electrospun polymer nanofibres with small diameters, Nanotechnology 17 (6) (2006) 1558.

[48] A.M. Al-Dhahebi, S.C.B. Gopinath, M.S.M. Saheed, Graphene impregnated electrospun nanofiber sensing materials: a comprehensive overview on bridging laboratory set-up to industry, Nano Converg. 7 (1) (2020) 27.

[49] H.-D. Huang, et al., Electrical conductivity and hydrophobicity of graphene oxide-modified carbon nanofibers, Chem. Phys. Lett. 771 (2021), 138551.

[50] Q. Zhang, et al., Graphene oxide-modified electrospun polyvinyl alcohol nanofibrous scaffolds with potential as skin wound dressings, RSC Adv. 7 (46) (2017) 28826-28836.

[51] G. Ghaderi, H. Tavanai, M. Bazarganipour, Electrospun graphene oxide incorporated PAN nanofibers, before and after activation, Mater. Res. Express 6 (10) (2019), 105047.

[52] G. Wang, et al., Synthesis of enhanced hydrophilic and hydrophobic graphene oxide nanosheets by a solvothermal method, Carbon 47 (1) (2009) 68-72.

[53] I.S. Raja, et al., The predominant factor influencing cellular behavior on electrospun nanofibrous scaffolds: wettability or surface morphology? Mater. Des. 216 (2022), 110580.

[54] J. Prakash, et al., In-vitro evaluation of electrospun cellulose acetate nanofiber containing graphene oxide/TiO2/curcumin for wound healing application, Colloids Surf. A Physicochem. Eng. Asp. 627 (2021), 127166.

[55] H.C. Kim, et al., High-strength cellulose nanofiber/graphene oxide hybrid filament made by continuous processing and its humidity monitoring, Sci. Rep. 11 (1) (2021) 13611.

[56] E. Sipos, A. Juhasz, M. Zrinyi, Characteristic load-elongation behavior of weak electrospun fiber texture, J. Mol. Liq. 329 (2021), 115459.

[57] K. Tanaka, et al., Development of an electrospinning method for the tensile testing of single nanofibers, High Performance Structures and Materials V, 2010, p. 177-+.

[58] M. ElMessiry, N. Fadel, The tensile properties of electrospun poly vinyl chloride and cellulose acetate (PVC/CA) bi-component polymers nanofibers, Alex. Eng. J. 58 (3) (2019) 885-890.

[59] C. Cao, et al., Nonlinear fracture toughness measurement and crack propagation resistance of functionalized graphene multilayers, Sci. Adv., 4(4), p. eaao7202.

[60] Y. Zhang, C. Zhang, Y. Wang, Recent progress in cellulose-based electrospun nanofibers as multifunctional materials, Nanoscale Adv. 3 (21) (2021) 6040-6047.

[61] E. Esmaeili, et al., The biomedical potential of cellulose acetate/polyurethane nanofibrous mats containing reduced graphene oxide/silver nanocomposites and curcumin: antimicrobial performance and cutaneous wound healing, Int. J. Biol. Macromol. 152 (2020) 418-427.

[62] J.J. Grant, et al., Biomedical applications of electrospun graphene oxide, ACS Biomater. Sci. Eng. 7 (4) (2021) 1278-1301.

[63] M.A. Kanjwal, A.A. Ghaferi, Graphene incorporated electrospun nanofiber for electrochemical sensing and biomedical applications: a critical review, Sensors 22 (2022) , **https://doi.org/10.3390/s22228661**.

[64] S. Prasadh, S. Suresh, R. Wong, Osteogenic potential of graphene in bone tissue engineering scaffolds, Materials 11 (2018), **https://doi.org/10.3390/ma11081430**.

[65] S. Faraji, et al., Electrospun poly-caprolactone/graphene oxide/quercetin nanofibrous scaffold for wound dressing: evaluation of biological and structural properties, Life Sci. 257 (2020), 118062.